VOLUME 114, NUMBER 16
JULY 29, 1992

JOURNAL
OF THE
AMERICAN
CHEMICAL
SOCIETY

Structural Characterization of the β-Bend Ribbon Spiral: Crystallographic Analysis of Two Long (L-Pro-Aib)$_n$ Sequential Peptides

B. Di Blasio,*[1a] V. Pavone,[1a] M. Saviano,[1a] A. Lombardi,[1a] F. Nastri,[1a] C. Pedone,[1a] E. Benedetti,[1a] M. Crisma,[1b] M. Anzolin,[1b] and C. Toniolo[1b]

Contribution from the Biocrystallography Center, CNR, Department of Chemistry, University of Naples, 80134 Naples, Italy, and the Biopolymer Research Center, CNR, Department of Organic Chemistry, University of Padova, 35131 Padova, Italy. *Received October 22, 1991*

Abstract: The molecular and crystal structures of two terminally blocked (L-Pro-Aib)$_n$ (n = 3, 4) sequential peptides were determined by X-ray diffraction. In both crystals two molecules in the asymmetric unit are found. Either molecule in the asymmetric unit of each structure shows a right-handed β-bend ribbon spiral, stabilized by the maximum possible number of intramolecular N–H···O=C H-bonds. Thus, for the first time it was possible to characterize at atomic resolution this polypeptide conformation.

Introduction

It has been suggested that in a sequential peptide the alternation of a conformationally restricted N-alkylated aminoacid residue, such as proline, which disrupts the conventional H-bonding schemes observed in helices, and a helix-forming residue, such as α-aminoisobutyric acid (Aib),[2] may give rise to a novel helical structure, called β-bend ribbon[3] (Figure 1). This structure may be considered as a subtype of the 3_{10}-helix,[4] having approximately the same helical fold of the peptide chain and being stabilized by 1 ← 4 (C_{10}) intramolecular N–H···O=C H-bonds.[5]

In this work we describe the complete structural characterization of this novel polypeptide conformation which may be of relevance in developing models for peptaibol antibiotics[6-8] and for the numerous (Pro-X)$_n$ (with X ≠ Pro) segments found in globular and fibrous proteins.[9-18] This result has been achieved by solving the X-ray diffraction structures of the two terminally blocked *p*BrBz-Aib-(L-Pro-Aib)$_n$-OMe (n = 3, 4) sequential peptides.

(1) (a) University of Naples. (b) University of Padova.
(2) Abbreviations: Aib, α-aminoisobutyric acid or $C^{\alpha,\alpha}$-dimethylglycine; *p*BrBz, *p*-bromobenzoyl; OMe, methoxy.
(3) Karle, I. L.; Flippen-Anderson, J.; Sukumar, M.; Balaram, P. *Proc. Natl. Acad. Sci. U.S.A.* **1987**, *84*, 5087–5091.
(4) Toniolo, C.; Benedetti, E. *TIBS* **1991**, *16*, 350–353.
(5) Toniolo, C. *CRC Crit. Rev. Biochem.* **1980**, *9*, 1–44.
(6) Benedetti, E.; Bavoso, A.; Di Blasio, B.; Pavone, V.; Pedone, C.; Toniolo, C.; Bonora, G. M. *Proc. Natl. Acad. Sci. U.S.A.* **1982**, *79*, 7951–7954.
(7) Brückner, H.; Graf, H. *Experientia* **1983**, *39*, 528–520.
(8) Mathew, M. K.; Balaram, P. *Mol. Cell. Biochem.* **1983**, *50*, 47–64.
(9) Umegane, T.; Maita, T.; Matsuda, G. *Hoppe-Seyler's Z. Physiol. Chem.* **1982**, *363*, 1321–1330.
(10) Quax-Jeuken, Y.; Janssen, C.; Quax, W.; van der Heuvel, R.; Bloemendal, H. *J. Mol. Biol.* **1984**, *180*, 457–472.
(11) Bhandari, D. G.; Levine, B. A.; Trayer, I. P.; Yeadon, M. E. *Eur. J. Biochem.* **1986**, *160*, 349–356.
(12) Schwarz, E.; Oesterhelt, D.; Reinke, H.; Beyreuther, K.; Dimroth, P. *J. Biol. Chem.* **1988**, *263*, 9640–9645.
(13) Wünsch, E.; Krois, D. *Monatsh. Chem.* **1989**, *120*, 1021–1028.
(14) Abillon, E.; Bremier, L.; Cardinaud, R. *Biochim. Biophys. Acta* **1990**, *1037*, 394–400.
(15) Kawamura, S.; Omoto, K.; Ueda, S. *J. Mol. Biol.* **1990**, *215*, 201–206.
(16) Brewer, S.; Tolley, M.; Trayer, I. P.; Barr, G. C.; Dorman, C. J.; Hannavy, K.; Higgins, C. F.; Evans, J. S.; Levine, B. A.; Wormald, M. R. *J. Mol. Biol.* **1990**, *216*, 883–895.
(17) Matsushima, N.; Creutz, C. E.; Kretsinger, R. H. *Proteins: Structure, Function, Genetics* **1990**, *7*, 125–155.
(18) Shewry, P. R.; Tatham, A. S. *Biochem. J.* **1990**, *267*, 1–12.

0002-7863/92/1514-6273$03.00/0

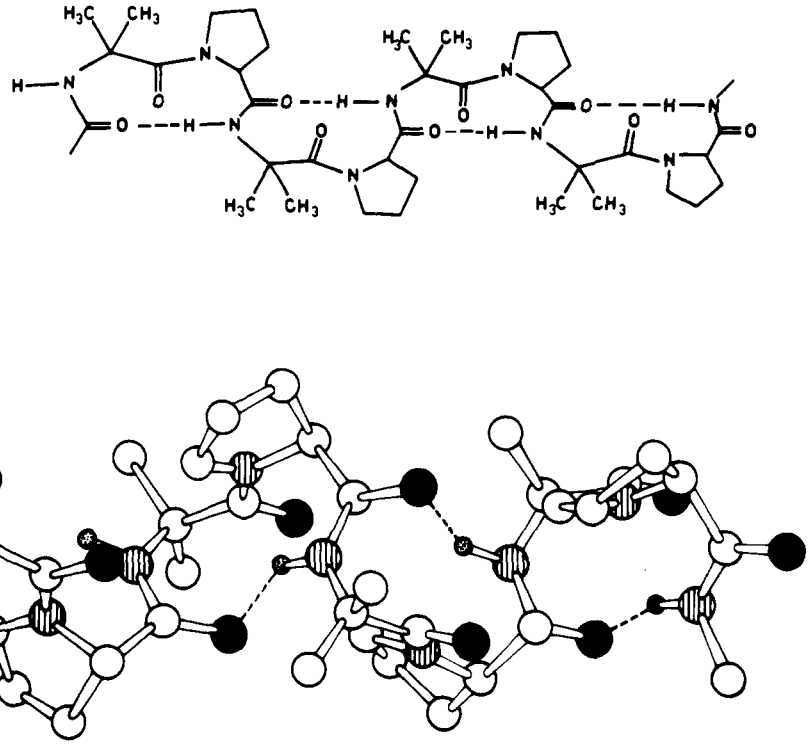

Figure 1. Two representations of the β-bend ribbon spiral generated by the repeating -L-Pro-Aib- dipeptide unit.

Experimental Section

Synthesis of Peptides. The synthesis and characterization of *p*BrBz-Aib-(L-Pro-Aib)$_n$-OMe (n = 3, 4) have been described elsewhere.[19]

X-ray Diffraction. Single crystals of *p*BrBz-Aib-(L-Pro-Aib)$_n$-OMe (n = 3, 4) were obtained from organic solutions in the form of colorless needles (Table I). Preliminary Weissenberg photographs were used to determine the crystal system and the space group. A CAD-4 Enraf-Nonius diffractometric system, equipped with PDP-8 and PDP-11 Digital computers, was used for determination of the unit cell constants, data collection, structure determination, and refinement. Crystallographic data for the two peptides are listed in Table I. In both crystals there are two molecules in the asymmetric unit.

The analysis of the peak profile suggested for both crystals an ω–2θ scan mode with a range of (1.1 + 0.20 tan θ)° for peak measurements; background counts were taken at both sides of each scan. A crystal-counter distance of 368 mm was used with a counter entrance aperture of 4 mm. A 200-mm long tube placed between the goniometer head and the detector was evacuated by using a vacuum pump. Prescan runs were made at a speed of 4°/min. Reflections with a net intensity $I \leq \sigma(I)0.5$ were flagged as "weak"; those with $I > \sigma(I)0.5$ were measured at lower speed in the range 1–4°/min, depending on the value $\sigma(I)/I$. The maximum time allowed for the scan was set to 60 s. Three intensity-control reflections were recorded every 60 min of X-ray exposure time; no significant change in their intensity was observed during data collection. A total of 9094 and 9813 independent reflections was measured for the hepta- and the nonapeptide, respectively. Intensity data were corrected for Lorentz and polarization factors. A total of 2230 and 3060 reflections for the hepta- and the nonapeptide, respectively, were considered "observed", having net intensity I greater than $3\sigma(I)$.

Both structures were solved by Patterson techniques and a nonstraightforward application of direct methods. The positions of the two independent bromine atoms in each structure were insufficient to determine the location of the remaining lighter atoms by Fourier techniques. Then, a starting set of phases heavily conditioned by the positions of the bromine atoms was determined. Its expansion by tangent formula brought to the determination of a partial structure in both the hepta- and the nonapeptide (in both cases about half of the atoms were located correctly in the cell). The positions of the remaining atoms of the two molecules in each crystal were determined by several successive difference Fourier maps. For the heptapeptide least-squares refinement with anisotropic thermal factors for all the Br, C, N, and O atoms were carried out, while for the nonapeptide structure only the bromine atoms were refined anisotropically. Hydrogen atoms were included in the final cycles of calculations in their stereochemically expected positions with isotropic thermal factors equal to the B equivalent of the carrier atom. The scattering factors for all atomic species were calculated from Cromer and Waber.[20] The heights of the highest and lowest values of the final ΔF map are 0.4, −0.3 e·Å^{-3} and 0.5, −0.4 e·Å^{-3}, respectively. All measurements and calculations were carried out at the Centro Interdipartimentale di Metodologie Chimico-fisiche of the University of Naples. The final values for the weighted R factor of the hepta- and the nonapeptide are 0.066 and 0.091, respectively. Tables of atomic coordinates, bond lengths and bond angles, and thermal parameters have been deposited as supplementary material.

Table I. Crystallographic Data for *p*BrBz-Aib-(L-Pro-Aib)$_n$-OMe (n = 3, 4)

parameter	*p*BrBz-Aib-(L-Pro-Aib)$_3$-OMe	*p*BrBz-Aib-(L-Pro-Aib)$_4$-OMe
molecular formula	$C_{39}H_{56}N_7O_9Br$	$C_{48}H_{70}N_9O_{11}Br$
molecular weight, amu	846.9	1029.1
crystal system	orthorhombic	orthorhombic
space group	$P2_12_12_1$	$P2_12_12_1$
Z, molecules/unit cell	8	8
a, Å	12.208 (8)	17.111 (6)
b, Å	21.363 (5)	20.745 (5)
c, Å	34.081 (3)	30.531 (3)
V, Å^3	8888.3	10837.5
d (exptl), g/cm^3	1.28	1.26
d (calcd), g/cm^3	1.28_1	1.26_1
radiation, Å	Cu Kα (1.5418)	Cu Kα (1.5418)
crystal size, mm	0.20 × 0.32 × 0.56	0.18 × 0.26 × 0.45
measd reflcns	9094	9813
reflcns with $I \geq 3\sigma(I)$	2230	3060
R factor	0.066	0.091
temp, °C	22	22
solvent of crystallization	CH_3OH	$(CH_3)_2CO/CH_3CH_2OH$ 1:1

(19) Crisma, M.; Anzolin, M.; Toniolo, C.; Pavone, V.; Di Blasio, B.; Saviano, M.; Lombardi, A.; Nastri, F.; Pedone, C.; Benedetti, E. *Gazz. Chim. Ital.*, in press.

(20) Cromer, D. T.; Waber, J. T. In *International Tables for X-ray Crystallography*; Kynoch Press: Birmingham, U.K., 1974; Vol. 4, Table 2.2.B.

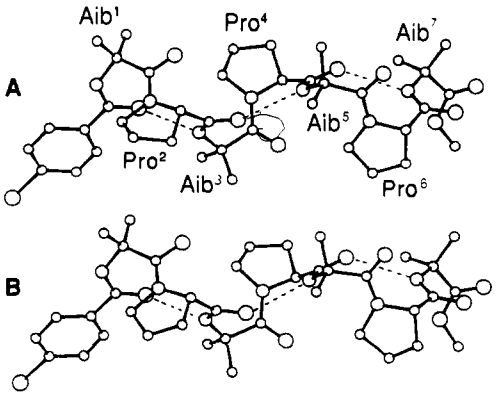

Figure 2. X-ray structures of molecules A and B of *p*BrBz-Aib-(L-Pro-Aib)$_3$-OMe with numbering of the atoms. The three intramolecular H-bonds are represented by dashed lines.

Table II. Selected Torsion Angles for *p*BrBz-Aib-(L-Pro-Aib)$_3$-OMe

A. Main-Chain Torsion Angles (deg) ($\sigma \approx 2.5°$)

angle	Aib¹	Pro²	Aib³	Pro⁴	Aib⁵	Pro⁶	Aib⁷
φ							
mol A	−47.7	−78.0	−56.6	−80.7	−46.9	−87.6	47.6
mol B	−54.4	−72.6	−63.5	−69.1	−48.5	−72.8	53.8
ψ							
mol A	−42.0	−14.5	−43.6	4.9	−46.3	4.2	45.1[a]
mol B	−36.1	−24.0	−28.1	−13.2	−45.6	−13.0	40.9[a]
ω							
mol A	−174.4	−164.3	−175.3	−171.2	−170.7	−179.2	−179.7[b]
mol B	−177.5	−164.4	177.8	−163.6	−172.9	−176.8	−176.8[b]

B. Proline Side-Chain Torsion Angles (deg) ($\sigma \approx 2.5°$)

	molecule A			molecule B		
torsion angle	Pro²	Pro⁴	Pro⁶	Pro²	Pro⁴	Pro⁶
$\theta(C'-N-C^\alpha-C^\beta)$	−8.3	−12.5	−15.8	0.1	3.2	−1.2
$\chi^1(N-C^\alpha-C^\beta-C^\gamma)$	13.8	−12.6	26.3	−20.6	−26.2	−6.4
$\chi^2(C^\alpha-C^\beta-C^\gamma-C^\delta)$	−15.1	31.8	−27.9	33.2	39.5	12.3
$\chi^3(C^\beta-C^\gamma-C^\delta-N)$	9.7	−38.9	16.9	−33.5	−37.4	−12.6
$\chi^4(C^\gamma-C^\delta-N-C^\alpha)$	−0.5	32.4	−0.1	21.3	22.2	7.8

puckering	molecule A			molecule B		
parameters[c]	Pro²	Pro⁴	Pro⁶	Pro²	Pro⁴	Pro⁶
Q	0.14	0.38	0.25	0.34	0.40	0.11
Φ	74°	304°	73°	286°	283°	293°
type of puckering[30]	C^γ-endo	C^γ-exo	C^γ-endo	C^γ-exo	C^γ-exo	C^γ-exo

C. Torsion Angles (deg) for the N- and C-Terminal Blocking Groups

	molecule A	molecule B
O(1)–C(7)–C(4)–C(3)	176.2	−176.7
O(1)–C(7)–C(4)–C(5)	−6.7	−0.4
N_1–C(7)–C(4)–C(3)	−4.7	4.8
N_1–C(7)–C(4)–C(5)	172.4	−178.9
C^α–N_1–C(7)–C(4)	−173.6	−173.2
N_7–C^α_7–C'_7–O_7	−134.7	−139.6

[a] N_7–C^α_7–C'_7–O_7*. [b] C^α_7–C'_7–O_7*–C(8). [c] As defined in ref 31.

Results and Discussion

The structures of the independent molecules A and B in the asymmetric unit of the terminally blocked sequential peptides *p*BrBz-Aib-(L-Pro-Aib)$_3$-OMe and *p*BrBz-Aib-(L-Pro-Aib)$_4$-OMe are shown in Figures 2 and 3, respectively. Tables II and III list the most relevant torsion angles. In Tables IV and V the intra- and intermolecular H-bonds are given. Figures 4 and 5 illustrate the modes of packing of the two structures.

Either molecule in the asymmetric unit of each peptide adopts a β-bend ribbon spiral structure. The helix screw sense in all molecules of the hepta- and the nonapeptide structures is right-handed, as expected on the basis of the L-chirality of the Pro residues. The β-bend ribbon in the heptapeptide is stabilized by three 1 ← 4 intramolecular H-bonds, occurring between the N–H

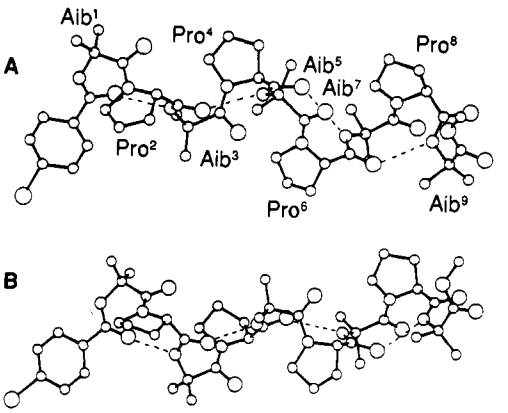

Figure 3. X-ray structures of molecules A and B of *p*BrBz-Aib-(L-Pro-Aib)$_4$-OMe with numbering of the atoms. The four intramolecular H-bonds are represented by dashed lines.

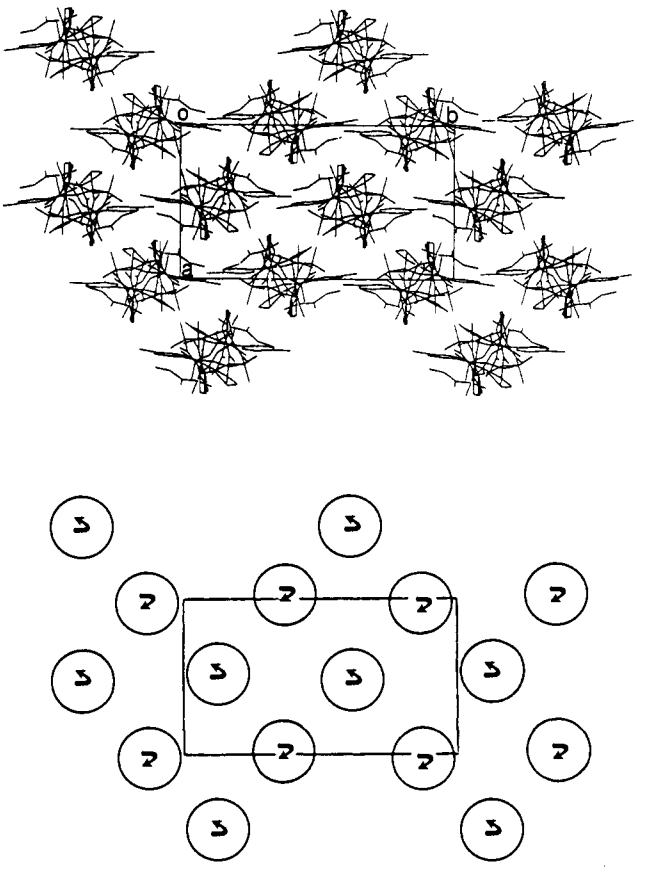

Figure 4. Mode of packing of the *p*BrBz-Aib-(L-Pro-Aib)$_3$-OMe molecules projected down the *c* axis, which corresponds to the β-bend ribbon axis. Along the helix axis A and B molecules are alternatively H-bonded one to the other, with formation of long rows. The curved arrow indicates the helix sense from the N- to the C-terminal of these rows. Layers of rows parallel to each other along the *ab* plane pack in an antiparallel fashion with adjacent layers.

groups of Aib³, Aib⁵, and Aib⁷ residues and the C=O groups of the *p*BrBz- moiety and of Pro² and Pro⁴ residues. The mean N···O distance is 2.98 Å.[21-23] Both independent nonapeptide molecules are stabilized by four 1 ← 4 intramolecular H-bonds, three of which occur between the same groups found in the heptapeptide structure, the fourth one being formed between the N–H group

(21) Ramakrishnan, C.; Prasad, N. *Int. J. Protein Res.* **1971**, *3*, 209–231.
(22) Taylor, R.; Kennard, O.; Versichel, W. *Acta Crystallogr., Sect. B* **1984**, *40*, 280–288.
(23) Görbitz, C. H. *Acta Crystallogr., Sect. B* **1989**, *45*, 390–395.

Table III. Selected Torsion Angles for *p*BrBz-Aib-(L-Pro-Aib)$_4$-OMe

A. Main-Chain Torsion Angles (deg) ($\sigma \approx 2.5°$)

angle	Aib^1	Pro^2	Aib^3	Pro^4	Aib^5	Pro^6	Aib^7	Pro^8	Aib^9
φ									
mol A	−53.1	−71.0	−59.8	−81.9	−48.5	−91.2	−50.8	−84.9	43.4
mol B	−47.7	−80.1	−52.6	−74.8	−58.2	−71.0	−66.3	−70.7	58.1
ψ									
mol A	−45.0	−23.2	−39.6	3.3	−42.5	11.7	−41.5	−13.3	38.3[a]
mol B	−36.9	−3.7	−39.3	−16.8	−39.8	−27.9	−27.4	−17.3	37.4[a]
ω									
mol A	−172.2	−165.7	−178.6	−168.2	−173.5	−174.5	−176.3	−167.4	179.1[b]
mol B	−173.2	−162.6	−171.1	−164.0	−174.4	−159.4	178.5	−176.6	−175.4[b]

B. Proline Side-Chain Torsion Angles (deg) ($\sigma \approx 2.5°$)

	molecule A				molecule B			
torsion angle	Pro^2	Pro^4	Pro^6	Pro^8	Pro^2	Pro^4	Pro^6	Pro^8
θ(C′–N–C$^\alpha$–C$^\beta$)	−11.0	−7.2	−18.5	−8.1	−6.3	−0.9	−9.0	−6.3
χ^1(N–C$^\alpha$–C$^\beta$–C$^\gamma$)	−10.9	27.2	27.2	−17.2	3.0	−16.8	32.0	30.9
χ^2(C$^\alpha$–C$^\beta$–C$^\gamma$–C$^\delta$)	29.0	−37.9	−25.9	36.0	1.5	30.5	−39.5	−44.4
χ^3(C$^\beta$–C$^\gamma$–C$^\delta$–N)	−36.0	31.9	13.6	−41.9	−5.3	−31.2	33.2	41.1
χ^4(C$^\gamma$–C$^\delta$–N–C$^\alpha$)	28.6	−16.0	3.6	32.2	7.2	19.2	−15.5	−22.3
puckering parameters[c]	molecule A				molecule B			
	Pro^2	Pro^4	Pro^6	Pro^8	Pro^2	Pro^4	Pro^6	Pro^8
Q	0.33	0.35	0.26	0.40	0.07	0.28	0.37	0.42
Φ	305°	98°	65°	298°	348°	289°	95°	278°
type of puckering[30]	C$^\gamma$-exo	C$^\gamma$-endo	C$^\gamma$-endo	C$^\gamma$-exo	planar	C$^\gamma$-exo	C$^\gamma$-endo	C$^\gamma$-exo

C. Torsion Angles (deg) for the N- and C-Terminal Blocking Groups

	molecule A	molecule B		molecule A	molecule B
O(1)–C(7)–C(4)–C(3)	−153.2	−142.5	N$_1$–C(7)–C(4)–C(5)	−144.3	−157.4
O(1)–C(7)–C(4)–C(5)	31.6	28.3	C$^\alpha$–N$_1$–C(7)–C(4)	−168.5	−179.0
N$_1$–C(7)–C(4)–C(3)	30.9	31.8	N$_9$–C$^\alpha_9$–C′$_9$–O$_9$	−14.5	−47.2

[a] N$_9$–C$^\alpha_9$–C′$_9$–O$_9$*. [b] C$^\alpha_9$–C′$_9$–O$_9$*–C(8). [c] As defined in ref 31.

of Aib^9 and the C=O group of Pro^6. The mean N···O distance is 3.00 Å.

As shown in Tables II and III, the backbone torsion angles φ, ψ, and ω for the two independent molecules of the heptapeptide are very similar, differing by no more than 15°. Conversely, those of the two independent molecules of the nonapeptide exhibit slightly larger differences, but they never exceed 30°. It is worth noting that, as found in most of the Aib-rich 3_{10}-helical peptide structures, the C-terminal Aib residue, whenever present, shows values for the φ, ψ angles pertaining to a helix with opposite handedness.[24-26]

For the first time, by taking advantage of the 14 independent -L-Pro-Aib- dipeptide units present in the hepta- and nonapeptide structures, we have been able to characterize at atomic resolution and β-bend ribbon structure. The average geometric and conformational parameters are given in Figure 6. It is worth mentioning that the φ, ψ angles of the Pro residue are to a considerable extent forced to the limits of the allowed conformational space (few Pro residues have values falling in the "bridge" region of the φ, ψ map[27]). This finding may be the result of the concerted variations observed in the bond angles of the peptide backbone[28,29] and of the deviations from planarity of the peptide bonds (in particular, the value for the Pro-Aib ω angle deviates considerably from the ideal trans 180° value). The required energy for these structural changes is partially regained by the formation of acceptable N–H···O=C H-bonds.

As shown in Tables II and III, both C$^\gamma$-endo and C$^\gamma$-exo pyrrolidine ring puckerings[30,31] are observed in each of the two pairs of independent molecules of the hepta- and the nonapeptide structures. This finding rules out the suggestion that this parameter would have a marked effect on backbone conformation and that only C$^\gamma$-endo puckered Pro residues could be accommodated in a β-bend ribbon spiral.[32]

The orientation of the N- and C-terminal blocking groups is defined by the torsion angles given in Tables II and III. The *p*BrBz moiety in the four independent observations shows almost the same conformation. The small differences observed (<40°) may be ascribed to the packing forces operative in the crystals. The C-terminal methoxy group adopts in all cases a conformation in which the O–CH$_3$ bond is staggered with respect to the C=O bond of the Aib residue.

The A and B helical molecules of *p*BrBz-Aib-(L-Pro-Aib)$_3$-OMe are held together in the crystal state by the formation of one intermolecular H-bond, as reported in Table IV. The N$_1$–H donor of each A molecule is H-bonded to the C′$_6$=O$_6$ acceptor group of a B molecule, and vice versa the N$_1$-H donor of each B molecule is H-bonded to the C′$_6$=O$_6$ acceptor group of an A molecule. This results in the formation of rows along the *c* axis of regularly alternating A and B molecules with the same helix sense. These rows pack with each other as shown in Figure 4.

In the case of *p*BrBz-Aib-(L-Pro-Aib)$_4$-OMe, A molecules are, by a simple translation along the *b* axis, intermolecularly H-bonded only to each other. B molecules behave similarly (Table V). The resulting long rows of A molecules and B molecules pack in the crystal as schematically reported in Figure 5: parallel to the *ab* plane, rows of A molecules pack in an antiparallel fashion to each other, while rows of B molecules pack in a parallel fashion. The

(24) Toniolo, C.; Bonora, G. M.; Bavoso, A.; Benedetti, E.; Di Blasio, B.; Pavone, V.; Pedone, C. *Biopolymers* **1983**, *22*, 205–215.
(25) Toniolo, C.; Benedetti, E. *ISI Atlas of Science: Biochemistry* **1988**, *1*, 225–230.
(26) Toniolo, C.; Benedetti, E. *Macromolecules* **1991**, *24*, 4004–4009.
(27) Zimmerman, S. S.; Pottle, M. S.; Némethy, G.; Scheraga, H. A. *Macromolecules* **1977**, *10*, 1–9.
(28) Benedetti, E. In *Chemistry and Biochemistry of Amino Acids, Peptides and Proteins*; Weinstein, B., Ed.; Dekker: New York, 1982; Vol. VI, pp 105–184.
(29) Nair, C. M. K.; Vijayan, M. *J. Indian Inst. Sci.* **1981**, *C63*, 81–103.
(30) Ashida, T.; Kakudo, M. *Bull. Chem. Soc. Jpn.* **1974**, *47*, 1129–1133.
(31) Cremer, D.; Pople, J. A. *J. Am. Chem. Soc.* **1975**, *97*, 1354–1358.
(32) Venkataram Prasad, B. V.; Balaram, P. *Int. J. Biol. Macromol.* **1982**, *4*, 99–102.

Table IV. Intra- and Intermolecular H-Bonds for *p*BrBz-Aib-(L-Pro-Aib)$_3$-OMe[a]

donor	acceptor	distance (Å)	angle (deg) N···O=C	symmetry operation
	A. Intramolecular H-Bonds			
N_3	O(1)	2.91	137	
		3.01	134	
N_5	O_2	3.00	131	
		3.08	134	
N_7	O_4	2.94	135	
		2.94	137	
	B. Intermolecular H-Bonds			
N_1(A)	O_6(B)	2.88	154	x, y, z
N_1(B)	O_6(A)	2.94	149	$x, y, z-1$

[a] Upper values, molecule A; lower values, molecule B.

Table V. Intra- and Intermolecular H-Bonds for *p*BrBz-Aib-(L-Pro-Aib)$_4$-OMe[a]

donor	acceptor	distance (Å)	angle (deg) N···O=C	symmetry operation
	A. Intramolecular H-Bonds			
N_3	O(1)	3.06	139	
		2.97	130	
N_5	O_2	3.00	125	
		3.00	140	
N_7	O_4	2.95	136	
		3.13	130	
N_9	O_6	2.88	128	
		3.04	134	
	B. Intermolecular H-Bonds			
N_1(A)	O_8(A)	2.99	144	$x, y+1, z$
N_1(B)	O_8(B)	2.94	138	$x, y+1, z$

[a] Upper values, molecule A; lower values, molecule B.

hexagonal packing of rows is such that each row is surrounded either by four parallel and two antiparallel rows or by two parallel and four antiparallel rows.

Conclusions

In this work for the first time we have characterized at atomic resolution a 3_{10}-helix subtype, the β-bend ribbon spiral, by solving the X-ray diffraction structures of two long (L-Pro-Aib)$_n$ sequential peptides. The repeating L-Pro-Aib dipeptide unit shows on the average the sequence of backbone torsion angles (φ_i, ψ_i, φ_{i+1}, ψ_{i+1}) −78°, −10°, −54°, and −40°. These values should be compared to those of a regular 3_{10}-helix: $\varphi_i = -57°$, $\psi_i = -30°$.[4] The mean helical parameters for the β-bend ribbon spiral are $n = 3.43$ amino acid residues per turn, h (axial translation per residue) = 2.06 Å, and p (pitch) = 7.07 Å, while the corresponding parameters for a regular 3_{10}-helix are $n = 3.24$, $h = 1.94$ Å, and $p = 6.29$ Å.[4]

In addition, the geometric and conformational parameters exhibited by *p*BrBz-Aib-(L-Pro-Aib)$_n$–OMe ($n = 3, 4$), described here, compare well with those found by X-ray diffraction analysis near the C-terminus of two zervamicin analogs[3,33] and in -L-Pro-Aib- containing short oligomers (from di- to tetrapeptides).[34-39]

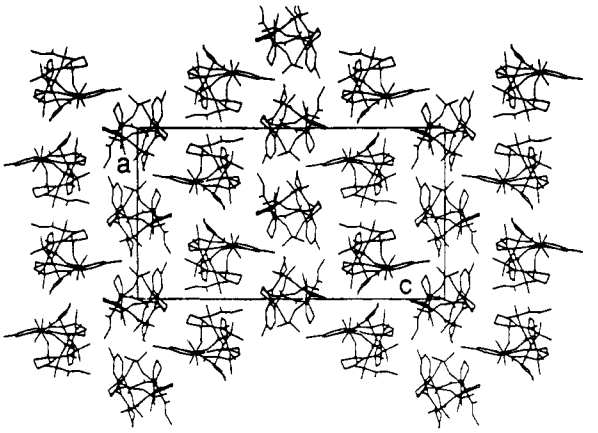

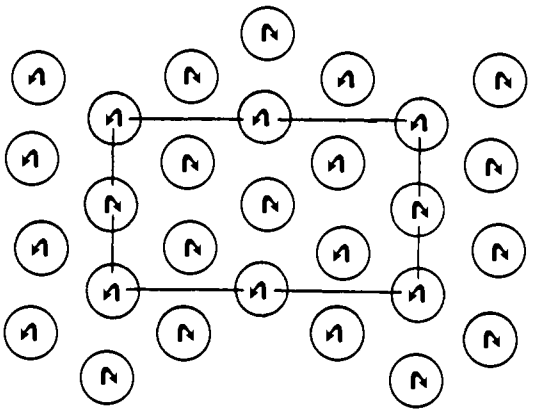

Figure 5. Mode of packing of the *p*BrBz-Aib-(L-Pro-Aib)$_4$-OMe molecules projected down the *b* axis, which corresponds to the β-bend ribbon axis. Along the helix axis A molecules are intermolecularly H-bonded only with each other. *B* molecules behave similarly. Thus, long rows of either A or B molecules occur along the *b* axis. The helix sense from the N- to the C-terminal of each row is indicated by the curved arrows. Parallel to the *ab* plane layers of isooriented rows (all having the same sense) pack with layers in which the rows have alternatively opposite sense.

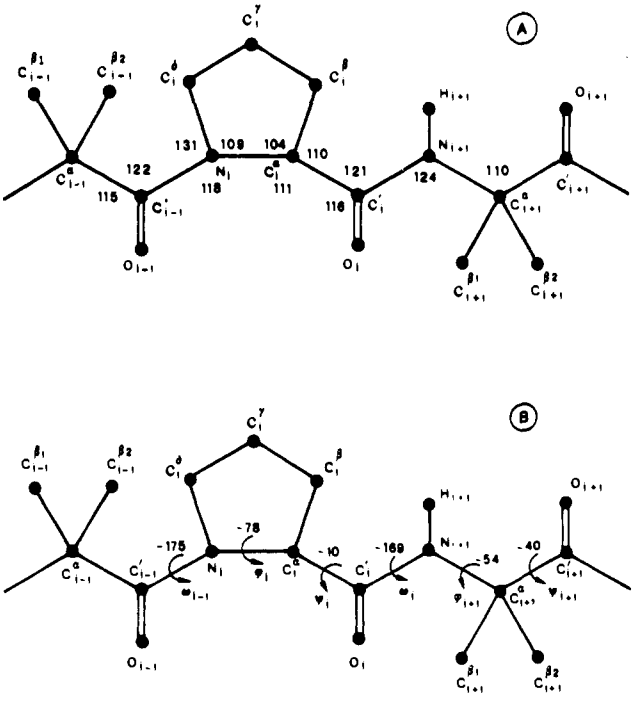

Figure 6. Average bond angles (A) and torsion angles (B) for the -Pro-Aib- dipeptide unit.

(33) Karle, I. L.; Flippen-Anderson, J. L.; Agarwalla, S.; Balaram, P. *Proc. Natl. Acad. Sci. U.S.A.* **1991**, *88*, 5307–5311.
(34) Venkataram Prasad, B. V.; Shamala, N.; Nagaraj, R.; Chandrasekharan, R.; Balaram, P. *Biopolymers* **1979**, *18*, 1635–1646.
(35) Venkatachalapathi, Y. V.; Nair, C. M. K.; Vijayan, M.; Balaram, P. *Biopolymers* **1981**, *20*, 1123–1136.
(36) Venkataram Prasad, B. V.; Balaram, H.; Balaram, P. *Biopolymers* **1982**, *21*, 1261–1273.
(37) Kawai, M.; Butsugan, Y.; Fukuyama, K.; Taga, T. *Biopolymers* **1987**, *26*, 83–94.
(38) Benedetti, E.; Bavoso, A.; Di Blasio, B.; Pavone, V.; Pedone, C.; Toniolo, C.; Bonora, G. M.; Crisma, M. *Int. J. Pept. Protein Res.* **1983**, *22*, 385–397.
(39) Valle, G.; Bardi, R.; Piazzesi, A. M.; Crisma, M.; Toniolo, C.; Cavicchioni, M.; Uma, K.; Balaram, P. *Biopolymers* **1991**, *31*, 1669–1676.

Acknowledgment. This research was supported in part by the Consiglio Nazionale delle Ricerche, Grant CTBCNR 89.5354. We also gratefully acknowledge the skillful technical assistance by Gabriella de Vita.

Registry No. *p*BrBz-Aib-(L-Pro-Aib)$_3$-OMe, 141613-74-3; *p*BrBz-Aib-(L-Pro-Aib)$_4$-OMe, 141613-75-4.

Supplementary Material Available: Tables of final atomic coordinates, bond lengths, and torsion angles for *p*BrBz-Aib-(L-Pro-Aib)$_3$-OMe and *p*BrBz-Aib-(L-Pro-Aib)$_4$-OMe (15 pages). Ordering information is given on any current masthead page.

On the Role of Individual Bleomycin Thiazoles in Oxygen Activation and DNA Cleavage

Norimitsu Hamamichi, Anand Natrajan, and Sidney M. Hecht*

Contribution from the Departments of Chemistry and Biology, University of Virginia, Charlottesville, Virginia 22901. *Received February 10, 1992*

Abstract: Two structurally novel bleomycin (BLM) analogs were prepared by total synthesis to permit the evaluation of the role of individual thiazole moieties in the processes of bleomycin-mediated oxygen activation and DNA degradation. Each of the compounds was structurally related to deglycobleomycin demethyl A_2 but contained an *S*-methyl-L-cysteine moiety in lieu of one of the two thiazoles normally present in bleomycin. In common with bleomycin and deglycobleomycin, both monothiazole BLMs were found to be excellent catalysts for the oxygenation of low molecular weight substrates such as naphthalene and styrene and also mediated the demethylation of *N*,*N*-dimethylaniline. However, both of the monothiazole BLMs were much less effective than bleomycin or deglycobleomycin in promoting DNA degradation. Analysis of the effects of the monothiazole BLMs on 5′- and 3′-^{32}P end labeled DNA duplexes indicated that cleavage occurred without discernible sequence selectivity. These results demonstrate that the bithiazole moiety in BLM is not required for O_2 activation or for the oxygenation and oxidation of low molecular substrates in what are presumably biomolecular processes. However, the bithiazole clearly does contribute to the efficiency of bleomycin-mediated DNA degradation and to the sequence selectivity of DNA strand scission by bleomycin.

The bleomycins are a family of structurally related, glycopeptide-derived antibiotics with significant antitumor activity.[1] Blenoxane, the clinically used mixture of bleomycins, contains bleomycin A_2 as its major constituent. The therapeutic effect of BLM is believed to result from its ability to mediate DNA degradation,[2,3] although it has been shown recently that BLM is also capable of mediating RNA degradation in a highly selective fashion.[4] The ability of BLM to degrade DNA is dependent on the participation of a redox-active metal ion cofactor such as Fe, Cu or Mn and a source of oxygen.[2,3,5] The ferrous ion–bleomycin complex, Fe(II)·BLM, combines with O_2 to produce a reactive and unstable oxygenated metallobleomycin species termed "activated bleomycin".[3,6] The available evidence suggests that activated Fe·BLM contains a high valent, metal–oxo species that is formed by 2e$^-$ reduction of Fe·BLM-bound oxygen to a peroxide, followed by heterolysis of the peroxide O–O bond.[6,7] Support for representation of activated Fe·BLM as a perferryl species derives from the similarities in the chemistry noted for activated

Chart I

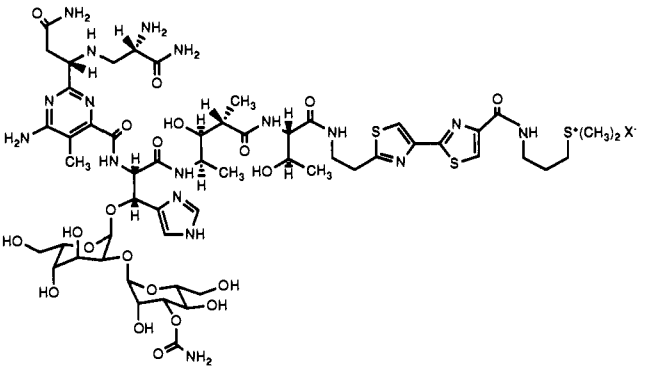

bleomycin A_2

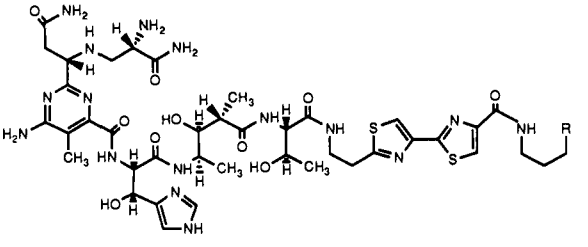

deglycobleomycin A_2 R = $S^+(CH_3)_2$

deglycobleomycin demethyl A_2 R = SCH_3

(1) (a) Umezawa, H. In *Bleomycin: Current Status and New Developments*; Carter, S. K., Crooke, S. T., Umezawa, H., Eds.; Academic Press: New York, 1978. (b) *Bleomycin: Chemical, Biochemical and Biological Aspects*; Hecht, S. M., Ed.; Springer-Verlag: New York, 1979. (c) Sugiura, Y.; Takita, T.; Umezawa, H. *Met. Ions. Biol. Syst.* **1985**, *19*, 81.

(2) (a) Ishida, R.; Takahashi, T. *Biochem. Biophys. Res. Commun.* **1975**, *66*, 1432. (b) Sausville, E. A.; Stein, R. W.; Peisach, J.; Horwitz, S. B. *Biochemistry* **1978**, *17*, 2740. (c) Sausville, E. A.; Stein, R. W.; Peisach, J.; Horwitz, S. B. *Biochemistry* **1978**, *17*, 2746.

(3) (a) Hecht, S. M. *Acc. Chem. Res.* **1986**, *19*, 83. (b) Kozarich, J. W.; Stubbe, J. *Chem. Rev.* **1987**, *87*, 1107.

(4) (a) Magliozzo, R. S.; Peisach, J.; Cirolo, M. R. *Mol. Pharmacol.* **1989**, *35*, 428. (b) Carter, B. J.; de Vroom, E.; Long, E. C.; van der Marel, G. A.; van Boom, J. H.; Hecht, S. M. *Proc. Natl. Acad. Sci. U.S.A.* **1990**, *87*, 9373. (c) Carter, B. J.; Holmes, C. E.; Van Atta, R. B.; Dange, V.; Hecht, S. M. *Nucleosides & Nucleotides* **1991**, *10*, 215. (d) Carter, B. J.; Reddy, K. S.; Hecht, S. M. *Tetrahedron* **1991**, *47*, 2463.

(5) (a) Dabrowiak, J. C. *Adv. Inorg. Chem.* **1982**, *4*, 70. (b) Petering, D. H.; Byrnes, R. W.; Antholine, W. E. *Chem.-Biol. Interact.* **1990**, *73*, 133.

(6) (a) Sugiura, Y.; Kikuchi, T. *J. Antibiot.* **1979**, *31*, 1310. (b) Burger, R. M.; Horwitz, S. B.; Peisach, J.; Wittenberg, J. B. *J. Biol. Chem.* **1979**, *254*, 1229. (c) Kuramochi, H.; Takahashi, K.; Takita, T.; Umezawa, H. *J. Antibiot.* **1981**, *34*, 576. (d) Burger, R. M.; Peisach, J.; Horwitz, S. B. *J. Biol. Chem.* **1981**, *256*, 11636.

0002-7863/92/1514-6278$03.00/0